Reconstructing spring sea ice concentration in the Chukchi Sea over recent centuries: insights into the application of the PIP$_{25}$ index

To cite this article: Jung-Hyun Kim *et al* 2019 *Environ. Res. Lett.* **14** 125004

View the article online for updates and enhancements.

Environmental Research Letters

LETTER

Reconstructing spring sea ice concentration in the Chukchi Sea over recent centuries: insights into the application of the PIP$_{25}$ index

Jung-Hyun Kim[1] , **Jong-Ku Gal**[1,2] , **Sang-Yoon Jun**[1], **Lukas Smik**[3], **Dahae Kim**[1], **Simon T Belt**[3], **Kwangkyu Park**[1], **Kyung-Hoon Shin**[2] and **Seung-Il Nam**[1]

1   Korea Polar Research Institute, 26 Songdomirae-ro, Yeonsu-gu, Incheon 21990, Republic of Korea
2   Department of Marine Science and Convergence Technology, Hanyang University ERICA campus, 55 Hanyangdaehak-ro, Sangnok-gu, Ansan-si, Gyeonggi-do 426-791, Republic of Korea
3   School of Geography, Earth and Environmental Sciences, University of Plymouth, Plymouth, PL4 8AA, United Kingdom

E-mail: jhkim123@kopri.re.kr

Abstract

In this study, we aimed to reconstruct spring (April–June) sea ice changes in the western Arctic Ocean over recent centuries (ca. the last 250 years) by measuring biomarker distributions in a multicore (ARA01B-03MUC) retrieved from the Chukchi Shelf region and to evaluate outcomes against known or modelled estimates of sea ice conditions. Specifically, we analyzed for the Arctic sea ice proxy IP$_{25}$ and assessed the suitability of a further highly branched isoprenoid (HBI) lipid (HBI III), epi-brassicasterol, and dinosterol as complementary biomarkers for use with the so-called phytoplankton marker-IP$_{25}$ index (PIP$_{25}$; P$_{III}$IP$_{25}$, P$_B$IP$_{25}$, and P$_D$IP$_{25}$, respectively). The presence of IP$_{25}$ throughout core ARA01B-03MUC confirms the occurrence of seasonal sea ice at the study site over recent centuries. From a semi-quantitative perspective, all three PIP$_{25}$ indices gave different trends, with some dependence on the balance factor c, a term used in the calculation of the PIP$_{25}$ index. P$_{III}$IP$_{25}$-derived spring sea ice concentration (SpSIC) estimates using a c value of 0.63, determined previously from analysis of Barents Sea surface sediments, were likely most reliable, since SpSIC values were high throughout the record (SpSIC > 78%), consistent with the modern context for the Chukchi Sea and the mean SpSIC record of the 41 CMIP5 climate models over recent centuries. P$_B$IP$_{25}$-based SpSIC estimates were also high (SpSIC 108%−127%), albeit somewhat over-estimated, when using a c value of 0.023 obtained from a pan-Arctic distribution of surface sediments. In contrast, P$_D$IP$_{25}$ values using a pan-Arctic c value of 0.11, and PIP$_{25}$ data based on the mean biomarker concentrations from ARA01B-03MUC, largely underestimated sea ice conditions (SpSIC as low as 13%), and exhibited poor agreement with instrumental records or model outputs. On the other hand, P$_B$IP$_{25}$ values using a c factor based on mean IP$_{25}$ and epi-brassicasterol concentrations exhibited a decline towards the core top, which resembled recent decreasing changes in summer sea ice conditions for the Chukchi Sea; however, further work is needed to test the broader spatial generality of this observation.

Introduction

Over the last four decades, the Arctic Ocean has experienced a persistent loss of sea ice, which is one of its main characteristics (e.g. Stroeve *et al* 2007, Serreze and Stroeve 2015). Such trends have been based mainly on satellite passive-microwave records spanning the last 40 years (e.g. de Vernal *et al* 2013), although some historical records extend back to ca. 1850 AD (e.g.

Walsh *et al* 2016). Such historical records have revealed seasonal variability, with the most profound sea ice reduction occurring in late summer (September), especially evident in the Chukchi Sea (western Arctic Ocean), even though winter (i.e. March) sea ice extent has remained largely unchanged in this region (Walsh *et al* 2016). Deciphering longer-term changes in sea ice on a seasonal and spatial basis remains a key aim in paleoclimatology.

A number of biogenic or geochemical proxies have been developed and applied to reconstruct sea ice conditions in the past (de Vernal *et al* 2013 and references therein). Amongst these is a mono-unsaturated highly branched isoprenoid (HBI) alkene (IP$_{25}$-Ice Proxy with 25 carbon atoms; Belt *et al* 2007), which is biosynthesized by certain Arctic sea ice dwelling diatoms during the spring bloom (Brown *et al* 2014) and, on sea ice melt, is deposited in underlying sediments (Belt *et al* 2007). Since its initial discovery, IP$_{25}$ has become an established northern hemisphere proxy for the qualitative occurrence of seasonal sea ice in various paleo records (e.g. Belt and Müller 2013, Belt 2018).

The absence of IP$_{25}$ in marine sediments has previously been considered to indicate either ice-free conditions or permanent ice cover (e.g. Belt *et al* 2007), although the validity of this simple two end-member interpretation still requires further investigation (Belt 2018). In any case, the co-measurement of IP$_{25}$ and various phytoplankton biomarkers was first proposed to differentiate between these end-members, since absent IP$_{25}$ but elevated phytoplankton biomarker concentrations would likely reflect ice-free conditions, while the absence (or very low abundance) of both biomarker types would be more consistent with intervals of permanent (or near permanent) ice cover (Müller *et al* 2009). Thereafter, Müller *et al* (2011) suggested combining IP$_{25}$ and open-water phytoplankton lipid biomarker concentrations in the form of a so-called phytoplankton marker-IP$_{25}$ index (PIP$_{25}$; see equation (3)). Importantly, the employment of this biomarker-based ratio method necessitates the use of a balance factor *c* (see equation (4)) to take account of the significant imbalance that often exists between IP$_{25}$ and phytoplankton biomarker concentrations (Müller *et al* 2011). The balance factor *c* is derived either from mean IP$_{25}$ and phytoplankton biomarker concentrations measured in an individual down-core sediment profile (e.g. Müller *et al* 2012, Cabedo-Sanz *et al* 2013) or is given as a fixed value, which can be obtained from a regional or pan-Arctic study of surface sediments (e.g. Xiao *et al* 2015, Smik *et al* 2016). However, the suitability of both approaches is in need of further investigation.

To date, three different PIP$_{25}$ have been used as indices for semi-quantitative proxy measures of sea ice change in some paleo sea ice reconstructions in the Arctic Ocean. These employ epi-brassicasterol (P$_B$IP$_{25}$, e.g. Müller *et al* 2011), dinosterol (P$_D$IP$_{25}$, e.g. Stoynova *et al* 2013), or a tri-unsaturated HBI (HBI III) (P$_{III}$IP$_{25}$, e.g. Belt *et al* 2015, Smik *et al* 2016) as the phytoplankton-derived biomarkers. According to Müller *et al* (2011), PIP$_{25}$ values greater than ca. 0.75 are indicative of extended sea ice cover, while values between 0.1 and 0.5 suggest variable or less ice cover. In the Barents Sea, surface sediment data exhibit a strong linear relationship between P$_{III}$IP$_{25}$ and spring sea ice concentration (SpSIC), with outcomes far less dependent on the balance factor *c* than for P$_B$IP$_{25}$

obtained from the same sediments (Smik *et al* 2016). This relationship, which uses a fixed, regional *c* value of 0.63, has been applied subsequently to obtain semi-quantitative estimates of SpSIC for the Barents Sea over Holocene and longer timeframes (Cabedo-Sanz and Belt 2016, Berben *et al* 2017, Köseoğlu *et al* 2018).
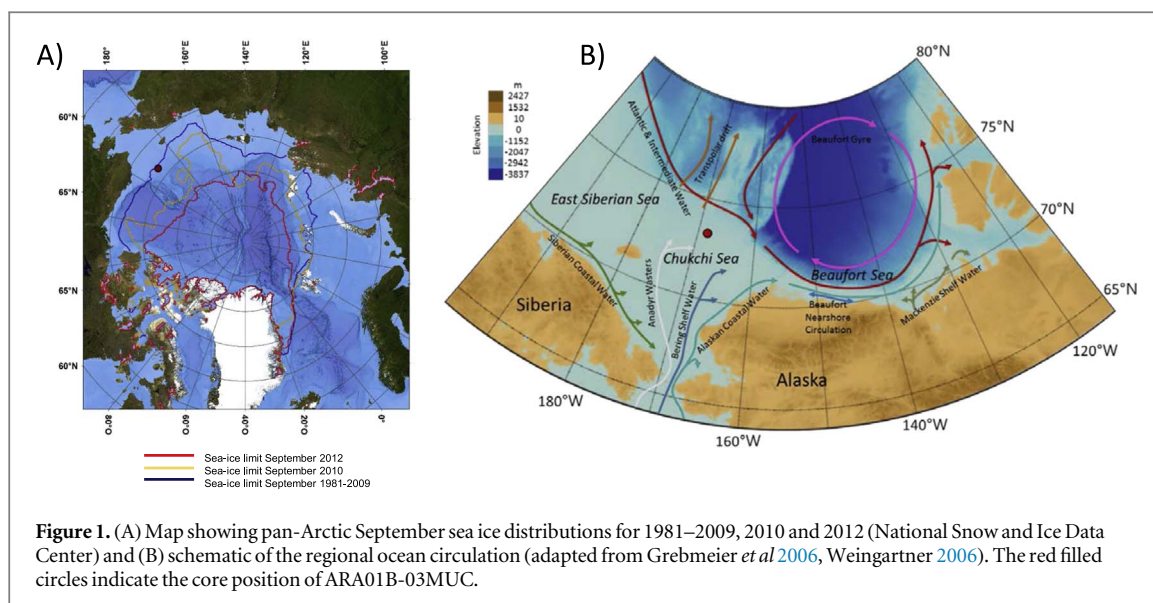
Notably, virtually all previous investigations into the use of the PIP$_{25}$ index have been based either on surface sediments, which are generally attributed to the most recent (years-decades) deposition, or down-core records spanning hundreds to millions of years (see Belt 2018 for a review). In contrast, relatively few studies have focused on IP$_{25}$ and other biomarker data in short cores representing recent decades-centuries, for which documented and high-resolution modelled sea ice records could be used for comparison, testing, and calibration purposes (Alonso-García *et al* 2013, Weckström *et al* 2013, Cormier *et al* 2016, Pieńkowski *et al* 2017). Further, only one such short core has previously been studied from a location (northern Barents Sea; Vare *et al* 2010, Köseoğlu *et al* 2018) with essentially uniform (and extensive) spring sea ice conditions against which corresponding consistency in biomarker data could be evaluated.

In the current study, we therefore measured IP$_{25}$, HBI III, epi-brassicasterol, and dinosterol concentrations in a multicore collected from a site in the Chukchi Sea and compared the corresponding PIP$_{25}$ records with other published sea ice records (Walsh *et al* 2016) and modelled sea ice properties in historical simulations from the Coupled Model Intercomparison Project (CMIP5; Taylor *et al* 2012). Since the core site is one that has experienced relatively constant spring sea ice conditions but declining summer sea ice extent over the most recent centuries, it provided a good opportunity to identify the most suitable biomarker-based proxy method for reconstructing such sea ice trends in the relatively recent past, but beyond that of surface sediments. In doing so, we further show the potential of the P$_{III}$IP$_{25}$ approach for subsequent application to paleo sea ice reconstruction in longer-term records.

Material and methods

Sample collection
Sediment core ARA01B-03MUC (23 cm long) was recovered from the shelf of the Chukchi Sea (73.52°N, 168.94°W, 72.5 m water depth) during the 2010 R/V ARAON Expedition (ARA01B) using a MUC 8 multi-corer developed by Oktopus GmbH (figure 1(A)). The study site is influenced by Pacific waters flowing northwards across the Chukchi Shelf along three principal pathways associated with major topographic depressions in the western, eastern, and central Chukchi Sea: more saline (>32.5), nutrient-rich Anadyr Water, fresher (<31.8), more nutrient-limited Alaska Coastal Water, and intermediate salinity

Figure 1. (A) Map showing pan-Arctic September sea ice distributions for 1981–2009, 2010 and 2012 (National Snow and Ice Data Center) and (B) schematic of the regional ocean circulation (adapted from Grebmeier *et al* 2006, Weingartner 2006). The red filled circles indicate the core position of ARA01B-03MUC.

(31.8–32.5) Bering Shelf Water (e.g. Grebmeier *et al* 2006 and references therein; figure 1(B)). According to recent satellite observations, sea ice covers most of the Chukchi Sea from December to May, and retreats during summer with a minimum value of less than $0.6 \times 10^6 \, \text{km}^2$ in September. In recent decades, sea ice concentration has especially decreased from July to November (Onarheim *et al* 2018). The sediments of core ARA01B-03MUC consist of olive-gray clayey silt. The sediment core was sectioned at 1 cm intervals (and a further section at 0.5 cm) on board and stored at $-20\,^\circ$C until further treatment.

Radioisotope analyses

Sub-samples (1 cm intervals) were indirectly measured for ^{210}Pb activity ($t_{1/2} = 22.23 \pm 0.12$ year) using the ^{210}Po method (Robbins and Edgington 1975, Nittrouer *et al* 1979) with an SSB alpha spectrometer (Canberra Inc., PIPS) at the Korea Basic Science Institute (South Korea). The analytical error is on average $2.3 \pm 0.8 \, \text{mBq g}^{-1}$ (figure 2). Excess ^{210}Pb activities (^{210}Pb$_{ex}$) were calculated by subtraction of supported level values (^{210}Pb$_{sup}$) from total activity (^{210}Pb$_{total}$). The apparent sedimentation rate (cm yr^{-1}) was calculated from ^{210}Pb$_{ex}$ using the constant flux and constant sediment accumulation rate model based on a slope of the logarithmic regression line (figure 2) as follows:

$$\text{Apparent sedimentation rate} = -\lambda/b \, (\text{cm yr}^{-1}), \tag{1}$$

where λ is the radioisotope decay constant (^{210}Pb, 0.031 14 per year) and b is the slope of the regression line.

Bulk geochemical analyses

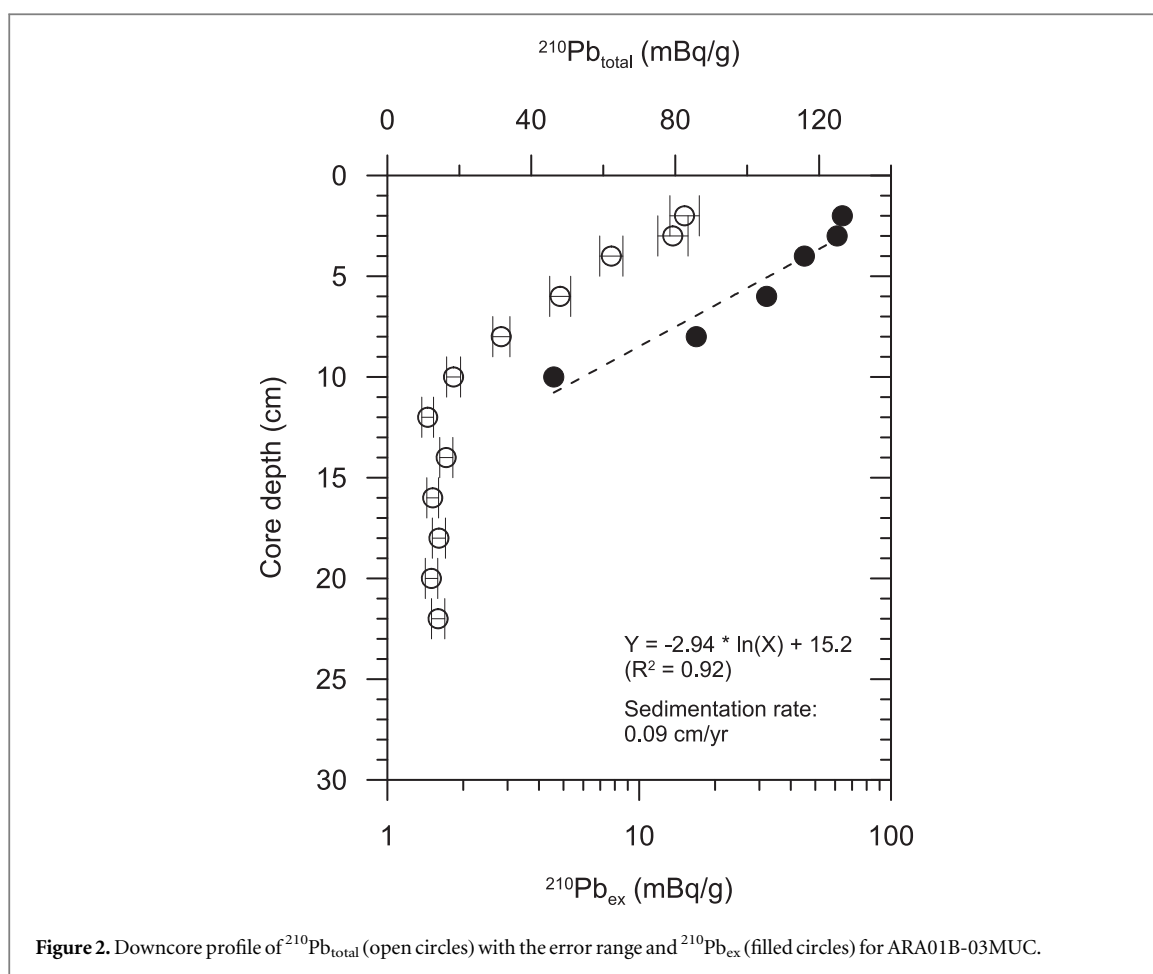Total carbon (TC) and total organic carbon (TOC) were determined at the Korea Polar Research Institute (South Korea) using a Flash 2000 organic elemental analyzer connected to a Delta V Plus isotope ratio mass spectrometer (Thermo Fisher Scientific). The samples were treated with HCl (10%) in order to remove carbonates prior to TOC analysis. The final TOC value was calculated using equation (2) (Stein *et al* 1994):

$$\text{TOC (wt\%)} = \frac{[100 - (8.333 \times \text{TC})]}{[(100/\text{TOC}') - 8.333]}. \tag{2}$$

The analytical error was less than ±0.1 wt% for TOC content.

Lipid biomarker analyses

Lipid analyses were conducted at the University of Plymouth (UK) according to Belt *et al* (2012). Briefly, freeze-dried sediments (ca. 1–2 g) were extracted by sonication (dichloromethane (DCM):methanol (MeOH); 2:1 v:v, 3 × 3 ml), and partially purified to remove polar components and elemental sulphur using tetrabutylammonium (TBA) sulfite reagent. Internal standards (9-octylheptadec-8-ene: 9-OHD and 5-α-androstan-3β-ol; 0.01 μg) were added prior to extraction for the quantification of HBIs and sterols, respectively. The total extracts were separated into apolar (HBIs) and polar (sterols) fractions using hexane and DCM:MeOH (1:1, v:v), respectively. HBIs and sterols were analyzed using gas chromatography–mass spectrometry (GC–MS) with conditions described elsewhere (Belt *et al* 2012). The polar fractions were derivatized using N,O-bis(trimethylsilyl)trifluoroacetamide (BSTFA) prior to the GC–MS analysis. Individual compounds were identified by total ion current (TIC; m/z 50–500 mass range) chromatograms, while selective ion monitoring chromatograms were used to quantify the abundances of HBI III (m/z 346), IP$_{25}$ (m/z 350), epi-brassicasterol (m/z 470), and dinosterol (m/z 500). The different response factors (RFs) were applied to account for the differences in mass spectral responses of selected compounds and the internal standards. However, dinosterol

Figure 2. Downcore profile of $^{210}Pb_{total}$ (open circles) with the error range and $^{210}Pb_{ex}$ (filled circles) for ARA01B-03MUC.

concentrations were obtained by only correcting the selected ion contributions to the total ion counts of 5-α-androstan-3β-ol and dinosterol identified in a reference sample.

PIP$_{25}$ indices based on HBI III, epi-brassicasterol, and dinosterol (i.e. P$_{III}$IP$_{25}$, P$_B$IP$_{25}$, and P$_D$IP$_{25}$) were calculated according to Müller *et al* (2011) using equations (3) and (4):

$$PIP_{25} = \frac{[IP_{25}]}{[IP_{25}] + [\text{phytoplankton biomarker} \times c]}$$
(3)

$$c = \frac{[\text{mean } IP_{25} \text{ concentration}]}{[\text{mean phytoplankton biomarker concentration}]}.$$
(4)

PIP$_{25}$ calculations using balance factor c values obtained from surface sediment calibrations from the Barents Sea (Smik *et al* 2016) and pan-Arctic locations (Xiao *et al* 2015) were also carried out (table 1).

Climate model simulations
Sea ice concentrations and sea ice thicknesses in the CMIP5 historical runs by 41 climate models for the period from AD 1862 to AD 2004 were used for comparing modelled sea ice properties with the proxy records. The CMIP5 historical runs were performed by coupled climate models to simulate observed climate changes during the 20th century, with forcing

of observed atmospheric composite changes from the nineteenth century to near present (Taylor *et al* 2012).

Results

^{210}Pb geochronology
The depth profile of excess ^{210}Pb is presented in figure 2. Measured $^{210}Pb_{total}$ activities ranged from 20 to 87 mBq g^{-1} of dry sediment weight, and $^{210}Pb_{sup}$ between 12 and 23 cm had an average value of 22.5 $\pm$ 1.6 mBq g^{-1} (figure 2). The concentration of excess ^{210}Pb decreased nearly exponentially with sediment depth. The mean sedimentation rate for core ARA01B-3MUC was 0.09 cm yr^{-1} ($R^2 = 0.92$), corresponding to a ca. 250 year record.
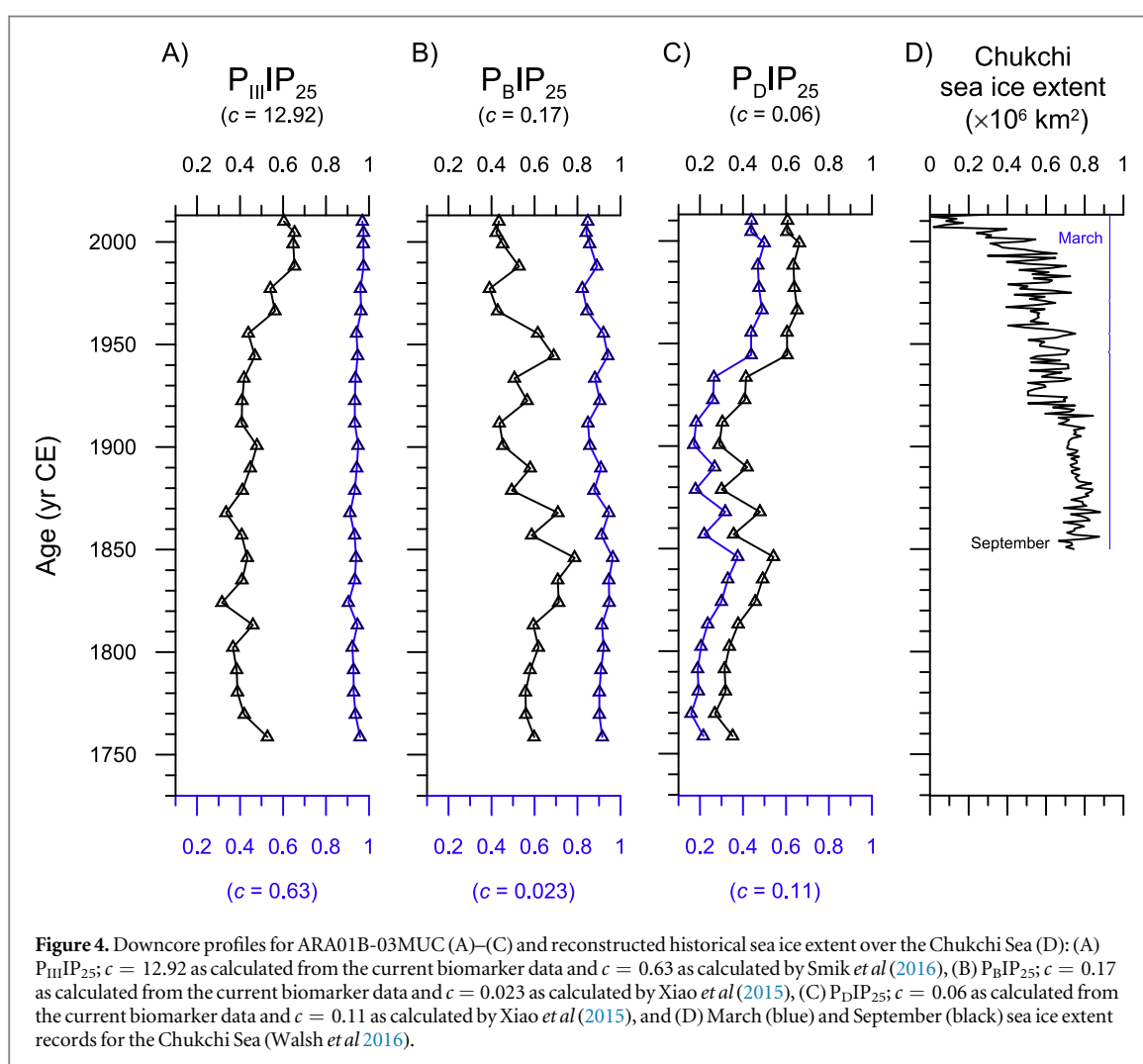
Proxy data
The TOC content varied between 1.6 and 2.3 wt% (table 1, figure 3). IP$_{25}$ was detected throughout core ARA01B-3MUC with variable concentration (0.3–2.6 μg g^{-1} TOC) and highest values towards the core top (table 1, figure 3). The HBI III (0.03–0.15 μg g^{-1} TOC) and epi-brassicasterol (1.0–21.3 μg g^{-1} TOC) concentration profiles were similar to that of IP$_{25}$. However, variation in dinosterol concentration (8.9–28.6 μg g^{-1} TOC) was different from the other two phytoplankton biomarkers. The c factors calculated from the sediment downcore data ($n = 25$) were

Table 1. TOC contents, biomarker concentrations, and PIP_{25} data obtained from ARA01B-03MUC.

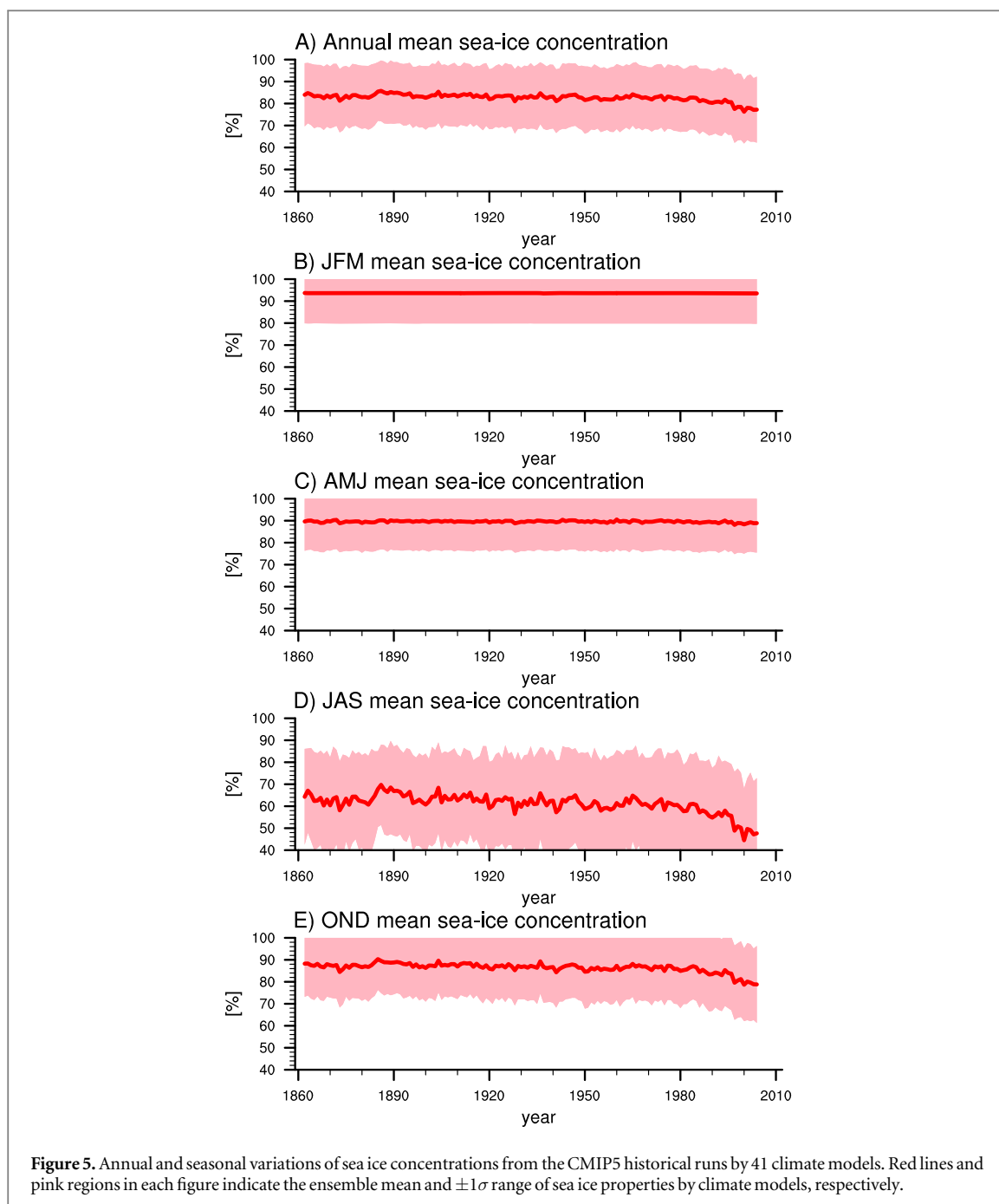| Core depth (cm)	Age (yr CE)	TOC (wt%)	IP_{25} ($\mu g\ g^{-1}$ TOC)	HBI III ($\mu g\ g^{-1}$ TOC)	Epi-brassicasterol ($\mu g\ g^{-1}$ TOC)	Dinosterol ($\mu g\ g^{-1}$ TOC)	$P_{III}IP_{25}$ ($c = 12.92$[a])	$P_{III}IP_{25}$ ($c = 0.63$[b])	$P_{B}P_{25}$ ($c = 0.17$[a])	$P_{B}IP_{25}$ ($c = 0.023$[c])	$P_{D}IP_{25}$ ($c = 0.06$[a])	$P_{D}IP_{25}$ ($c = 0.11$[c])
0	2010	3.3	1.9	0.10	14.9	22.1	0.60	0.97	0.43	0.85	0.61	0.44
0.5	2005	3.4	1.6	0.07	13.2	18.7	0.65	0.97	0.42	0.84	0.60	0.44
1	1999	2.9	2.6	0.11	18.7	23.4	0.65	0.97	0.45	0.86	0.66	0.50
2	1988	2.9	2.4	0.10	12.9	24.8	0.65	0.97	0.53	0.89	0.63	0.47
3	1977	2.6	2.3	0.15	21.3	22.9	0.54	0.96	0.39	0.82	0.64	0.47
4	1966	2.6	1.8	0.11	14.6	17.4	0.56	0.96	0.43	0.84	0.65	0.49
5	1955	2.5	1.2	0.12	4.6	14.4	0.44	0.94	0.62	0.92	0.60	0.44
6	1944	2.4	1.3	0.11	3.5	15.2	0.47	0.95	0.69	0.94	0.61	0.44
7	1933	2.3	1.0	0.11	5.8	24.9	0.42	0.94	0.51	0.88	0.41	0.26
8	1923	2.3	0.7	0.08	3.2	18.1	0.41	0.93	0.57	0.90	0.41	0.26
9	1912	2.3	0.7	0.08	5.4	28.6	0.41	0.93	0.44	0.85	0.30	0.18
10	1901	2.4	0.6	0.05	4.3	26.6	0.48	0.95	0.45	0.86	0.29	0.17
11	1890	2.3	0.6	0.06	2.5	14.5	0.45	0.94	0.58	0.91	0.42	0.27
12	1879	2.1	0.5	0.06	3.3	22.7	0.41	0.93	0.49	0.88	0.30	0.18
13	1868	2.3	0.6	0.09	1.4	11.1	0.33	0.91	0.71	0.95	0.48	0.32
14	1857	2.2	0.7	0.08	2.8	21.6	0.41	0.93	0.59	0.91	0.36	0.22
15	1846	2.3	0.6	0.06	1.0	9.4	0.43	0.94	0.79	0.96	0.54	0.38
16	1835	2.3	0.5	0.05	1.2	8.9	0.41	0.93	0.71	0.95	0.49	0.33
17	1824	2.2	0.4	0.07	1.0	9.1	0.32	0.90	0.71	0.95	0.46	0.30
18	1813	2.3	0.4	0.03	1.6	11.3	0.46	0.95	0.59	0.91	0.38	0.24
19	1802	2.4	0.3	0.04	1.2	11.0	0.37	0.92	0.62	0.92	0.34	0.20
20	1791	2.1	0.3	0.04	1.4	12.3	0.38	0.93	0.58	0.91	0.31	0.19
21	1780	2.1	0.4	0.04	1.7	13.7	0.39	0.93	0.56	0.90	0.32	0.19
22	1769	2.4	0.3	0.03	1.4	13.9	0.42	0.94	0.56	0.90	0.27	0.16
23	1759	2.2	0.4	0.03	1.8	14.7	0.53	0.96	0.60	0.92	0.35	0.22

[a] Indicates this study.

[b] Smik *et al* (2016).

[c] Xiao *et al* (2015).

Figure 3. Downcore profiles of the concentrations of (A) TOC (wt%), (B) IP_{25}, (C) HBI III, (D) epi-brassicasterol, and (E) dinosterol for ARA01B-03MUC. The areas above the mean core concentration values for each biomarker are shaded in grey.

Figure 4. Downcore profiles for ARA01B-03MUC (A)–(C) and reconstructed historical sea ice extent over the Chukchi Sea (D): (A) $P_{III}IP_{25}$; $c = 12.92$ as calculated from the current biomarker data and $c = 0.63$ as calculated by Smik *et al* (2016), (B) $P_{B}IP_{25}$; $c = 0.17$ as calculated from the current biomarker data and $c = 0.023$ as calculated by Xiao *et al* (2015), (C) $P_{D}IP_{25}$; $c = 0.06$ as calculated from the current biomarker data and $c = 0.11$ as calculated by Xiao *et al* (2015), and (D) March (blue) and September (black) sea ice extent records for the Chukchi Sea (Walsh *et al* 2016).

12.92 for HBI III, 0.17 for epi-brassicasterol, and 0.06 for dinosterol. The resulting $P_{III}IP_{25}$, $P_{B}IP_{25}$, and $P_{D}IP_{25}$ indices were in the ranges 0.3–0.7, 0.4–0.8 and

0.3–0.7, respectively (figure 4). The $P_{III}IP_{25}$ and $P_{D}IP_{25}$ trends were similar, with higher values towards the core top; however, the $P_{B}IP_{25}$ record showed a

Figure 5. Annual and seasonal variations of sea ice concentrations from the CMIP5 historical runs by 41 climate models. Red lines and pink regions in each figure indicate the ensemble mean and $\pm 1\sigma$ range of sea ice properties by climate models, respectively.

decreasing trend during the same period. On the other hand, $P_{III}IP_{25}$ and $P_{B}IP_{25}$ values were consistently >0.8 when using c values of 0.63 and 0.023, determined from previous surface sediment calibrations from the Barents Sea and pan-Arctic locations, respectively (figures 4(A) and (B); Xiao *et al* 2015, Smik *et al* 2016). However, $P_{D}IP_{25}$ values using the pan-Arctic c value of 0.11 for dinosterol (Xiao *et al* 2015) were even lower than those obtained using the current core biomarker data (figure 4(C)).

Model data

The ensemble mean of annual sea ice concentrations of the CMIP5 models averaged over the region of the Chukchi Sea (70–80°N and 150°E–150°W) showed a gradual decrease from around AD 1980 (figure 5). Notably, the winter (January–March) and spring (April–June) mean sea ice concentrations remained high ($>96\%$ and $>90\%$, respectively), whilst, after around AD 1980, the sea ice concentrations decreased noticeably in summer (July–September) and autumn (October–December).

Discussion

The sedimentation rate (0.09 cm yr^{-1}) obtained at our core site falls within the range reported for other sediment cores from the Chukchi Shelf (0.03−0.37 cm yr^{-1};
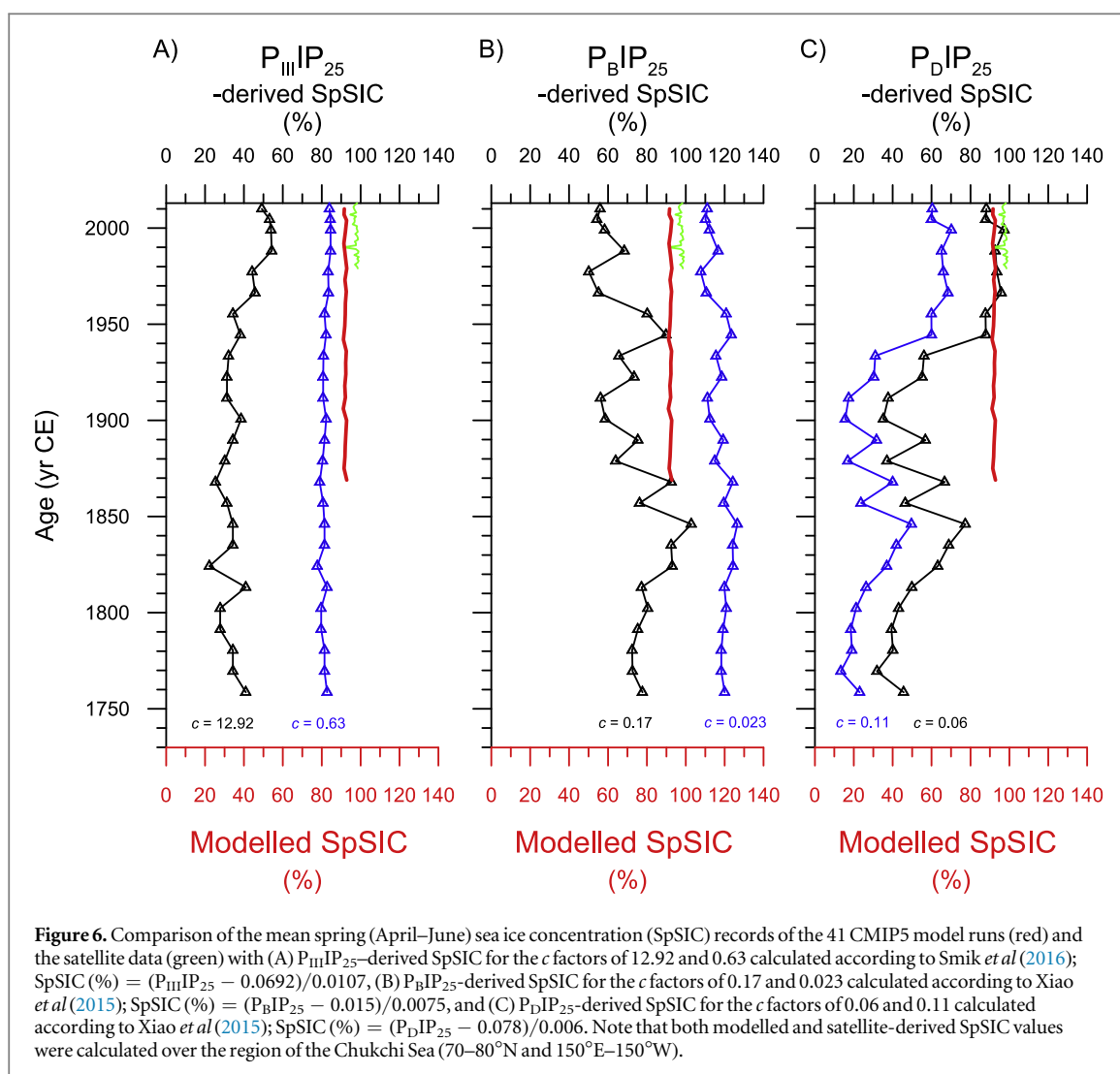
Cooper and Grebmeier 2018), for the Beaufort Shelf ($0.14\,cm\,yr^{-1}$; Bringué and Rochon 2012), and on the Beaufort Sea slope ($0.10-0.20\,cm\,yr^{-1}$; Kuzyk *et al* 2013). The nearly exponential decrease of the excess ^{210}Pb suggests that mixing by bioturbation and/or physical processes was minor at our core site. Nonetheless, it should be noted that the Chukchi Shelf can have a significant degree of bioturbation due to high benthic macrofaunal populations and biomass. For example, Kuzyk *et al* (2013) reported surface mixed layers of 10–30 cm on the Chukchi Shelf (<200 m water depth). However, previously published data from a sediment core (73.36°N, 175.62°W) geographically closest to our core site (73.52°N, 168.94°W), has similar sedimentation rates of 0.06 and $0.08\,cm\,yr^{-1}$ using ^{210}Pb and ^{137}Cs, respectively (Cooper and Grebmeier 2018). Accordingly, it appears that our core site is located far enough north that the more southerly observations of bioturbation on the Chukchi Shelf may not be so significant.

The presence of IP_{25} throughout core ARA01B-03MUC (figure 3) provides proxy evidence for seasonal sea ice occurrence at the core site over recent centuries. The IP_{25} concentration of the core top sample ($1.9\,\mu g\,g^{-1}$ TOC) was at the lower end of values ($3.6 \pm 1.9\,\mu g\,g^{-1}$ TOC) found previously in surface sediments from the Chukchi Plateau near to our Chukchi Shelf core site (Xiao *et al* 2015). The phytoplankton biomarker concentrations of the core top sample (14.9 and $22.1\,\mu g\,g^{-1}$ TOC for epi-brassicasterol and dinosterol, respectively) were also of the same order of magnitude to those from the Chukchi Plateau (77 ± 34 and $37 \pm 12\,\mu g\,g^{-1}$ TOC for epi-brassicasterol and dinosterol, respectively), even though the epi-brassicasterol concentrations were slightly lower (Xiao *et al* 2015). The HBI III concentrations were not reported in the previous analyses of Chukchi Sea sediments (Stoynova *et al* 2013, Xiao *et al* 2015, Polyak *et al* 2016, Stein *et al* 2017), although values in ARA01B-03MUC ($1-4\,ng\,g^{-1}$) were within the range of those ($0.1-30\,\mu g\,g^{-1}$) reported in surface sediments from the Barents Sea (e.g. Belt *et al* 2015, Smik *et al* 2016). More recently, Bai *et al* (2019) investigated surface sediments in the Chukchi Sea, reporting HBI III concentrations of $0.01-0.91\,\mu g\,g^{-1}$ TOC. However, the values of Bai *et al* (2019) cannot be compared directly with our data since, unfortunately, no instrumental RFs were used by Bai *et al* (2019) when calculating biomarker concentrations. Most significantly, the trend in IP_{25} concentration recorded in our Chukchi Shelf core did not reflect the near-uniform spring sea ice conditions for the Chukchi Sea over recent centuries (figure 3).

The general trends of the three PIP_{25} records calculated using the *c* values based on the current sediment core data (i.e. using equation (4)) were dependent on the specific phytoplankton-derived biomarkers used (figure 4). Thus, while both $P_{III}IP_{25}$ and $P_{D}IP_{25}$ records showed an increasing sea ice trend towards the core-top (ca. recent decades), the $P_{B}IP_{25}$

values decreased over the same interval. However, in all three cases, only relatively few PIP_{25} values were above the proposed threshold (0.75; Müller *et al* 2011) indicative of the extensive sea ice cover that characterizes the core site, with many substantially lower (i.e. below 0.5; figure 4). In contrast, $P_{III}IP_{25}$ and $P_{B}IP_{25}$ values were all greater than 0.75 when using *c* values of 0.63 and 0.023 obtained from the Barents Sea (Smik *et al* 2016) and pan-Arctic (Xiao *et al* 2015) databases, respectively, indicative of extensive sea ice cover (Müller *et al* 2011), a well-known feature of the core site. Use of the pan-Arctic *c* value of 0.11 for $P_{D}IP_{25}$, however, gave consistently low values ($P_{D}IP_{25}$ ca. 0.2–0.5; figure 4), implying variable or low sea ice extent (Müller *et al* 2011) and, therefore, under-estimates of sea ice conditions at the core site. On the basis of these outcomes, the most reliable measures of spring sea ice concentration for the core site were derived from PIP_{25} values using IP_{25} and HBI III or epi-brassicasterol (but not dinosterol), and using fixed values for *c*. This conclusion is supported further through conversion of PIP_{25} data to estimates of SpSIC using the calibrations of Smik *et al* (2016) and Xiao *et al* (2015). Thus, $P_{III}IP_{25}$-derived SpSIC estimates were all >78% in close agreement with the modelled values (>90%) and those from satellite data (https://nsidc.org/data/nsidc-0051) in the modern era (figure 6). The corresponding $P_{B}IP_{25}$-derived SpSIC was, however, slightly over-estimated (108% −127%), while the $P_{D}IP_{25}$-derived values were mainly well below 50% (figure 6). As such, the closest agreement between biomarker-derived and modelled SpSIC over recent centuries was obtained using $P_{III}IP_{25}$ data based on IP_{25} and HBI III using a *c* value obtained from Barents Sea surface sediments (i.e. $c = 0.63$). Further refinement of the optimal absolute value of *c* for the Chukchi Sea might potentially be obtained through future and more accurate quantitative analysis of surface sediments from the study region.

Finally, we note that the only biomarker record that mimics the well-known pronounced reduction in late summer sea ice cover in the Chukchi Sea in recent decades (figure 4(D); Walsh *et al* 2016) was the $P_{B}IP_{25}$ profile using a value of *c* based on the core data (i.e. Figure 4(B); $c = 0.17$). Since some recently reported sediment trap data from the Chukchi Sea showed that the epi-brassicasterol flux was still relatively high in late summer, while the HBI III flux was reduced in summer compared to spring values (Bai *et al* 2019), it follows that certain sterols potentially integrate, to some degree, both spring and summer conditions. Accordingly, the major production of IP_{25} in sea ice and HBI III in open waters along the sea ice edge during the spring season appear to provide the most reliable biomarker pair for estimating PIP_{25}-derived SpSIC in the Chukchi Sea, while the additional use of $P_{B}IP_{25}$ may potentially provide complementary insights into subsequent summer sea ice trends.

Figure 6. Comparison of the mean spring (April–June) sea ice concentration (SpSIC) records of the 41 CMIP5 model runs (red) and the satellite data (green) with (A) $P_{III}IP_{25}$–derived SpSIC for the c factors of 12.92 and 0.63 calculated according to Smik *et al* (2016); SpSIC (%) = ($P_{III}IP_{25}$ − 0.0692)/0.0107, (B) P_BIP_{25}-derived SpSIC for the c factors of 0.17 and 0.023 calculated according to Xiao *et al* (2015); SpSIC (%) = (P_BIP_{25} − 0.015)/0.0075, and (C) P_DIP_{25}-derived SpSIC for the c factors of 0.06 and 0.11 calculated according to Xiao *et al* (2015); SpSIC (%) = (P_DIP_{25} − 0.078)/0.006. Note that both modelled and satellite-derived SpSIC values were calculated over the region of the Chukchi Sea (70–80°N and 150°E–150°W).

Conclusions

The northern hemisphere sea ice biomarker IP_{25} was present throughout multicore ARA01B-03MUC retrieved from the Chukchi Shelf, reflecting the occurrence of seasonal sea ice at the core site over recent centuries. PIP_{25} data were most consistent with the well-known (and modelled) relatively constant spring sea ice conditions over recent centuries when HBI III and epi-brassicasterol were employed as the phytoplankton counterparts to IP_{25}, and when using fixed values for the balance factor c obtained from some previous calibrations studies based on regional or pan-Arctic surface sediments. In contrast, PIP_{25} values based on IP_{25} and dinosterol, or by using c values for all three phytoplankton biomarkers obtained from the current core data, gave unrealistic and generally too low estimates of SpSIC. The resemblance of PIP_{25} data based on IP_{25} and epi-brassicasterol in ARA01B-03MUC to the recent summer sea ice decline potentially reflects the longer production season of this biomarker compared to HBI

III; however, this will require testing through further surface sediment and seasonal *in situ* water column analyses.

Acknowledgments

Data availability statement

Any data that support the findings of this study are included within the article.

ORCID iDs

Jung-Hyun Kim ⓘ https://orcid.org/0000-0003-4987-609X

Jong-Ku Gal ⓘ https://orcid.org/0000-0002-7455-1206

References

Alonso-García M, Andrews J T, Belt S T, Cabedo-Sanz P, Darby D and Jaeger J 2013 A comparison between multiproxy and historical data (AD 1990–1840) of drift ice conditions on the East Greenland Shelf (~66°N) *Holocene* **23** 1672–83

Bai Y *et al* 2019 Seasonal and spatial variability of sea ice and phytoplankton biomarker flux in the Chukchi sea (western Arctic Ocean) *Prog. Oceanog.* **171** 22–37

Belt S T 2018 Source-specific biomarkers as proxies for Arctic and Antarctic sea ice *Org. Geochem.* **125** 277–98

Belt S T, Brown T A, Rodriguez A N, Sanz P C, Tonkin A and Ingle R 2012 A reproducible method for the extraction, identification and quantification of the Arctic sea ice proxy IP_{25} from marine sediments *Anal. Methods* **4** 705

Belt S T, Cabedo-Sanz P, Smik L, Navarro-Rodriguez A, Berben S M P, Knies J and Husum K 2015 Identification of paleo Arctic winter sea ice limits and the marginal ice zone: optimised biomarker-based reconstructions of late quaternary Arctic sea ice *Earth Planet. Sci. Lett.* **431** 127–39

Belt S T, Massé G, Rowland S J, Poulin M, Michel C and LeBlanc B 2007 A novel chemical fossil of palaeo sea ice: IP_{25} *Org. Geochem.* **38** 16–27

Belt S T and Müller J 2013 The Arctic sea ice biomarker IP_{25}: a review of current understanding, recommendations for future research and applications in paleo sea ice reconstructions *Quat. Sci. Rev.* **79** 9–25

Berben S M P, Husum K, Navarro-Rodriguez A, Belt S T and Aagaard-Sørensen S 2017 Semi-quantitative reconstruction of early to late Holocene spring and summer sea ice conditions in the northern Barents sea *J. Quat. Sci.* **32** 587–603

Bringué M and Rochon A 2012 Late Holocene paleoceanography and climate variability over the Mackenzie slope (Beaufort sea, Canadian Arctic) *Mar. Geol.* **291–294** 83–96

Brown T A, Belt S T, Tatarek A and Mundy C J 2014 Source identification of the Arctic sea ice proxy IP_{25} *Nat. Commun.* **5** 4197

Cabedo-Sanz P and Belt S T 2016 Seasonal sea ice variability in eastern fram strait over the last 2000 years *Arktos* **2** 22

Cabedo-Sanz P, Belt S T, Knies J and Husum K 2013 Identification of contrasting seasonal sea ice conditions during the Younger Dryas *Quat. Sci. Rev.* **79** 74–86

Cooper L W and Grebmeier J M 2018 Deposition patterns on the Chukchi shelf using radionuclide inventories in relation to surface sediment characteristics *Deep-Sea Res.* II **152** 48–66

Cormier M-A, Rochon A, de Vernal A and Gélinas Y 2016 Multi-proxy study of primary production and paleoceanographical conditions in northern Baffin Bay during the last centuries *Mar. Micropaleontol.* **127** 1–10

de Vernal A, Gersonde R, Goosse H, Seidenkrantz M and Wolff E W 2013 Sea ice in the paleoclimate system: the challenge of reconstructing sea ice from proxies: an introduction *Quat. Sci. Rev.* **79** 1–8

Grebmeier J M, Cooper L W, Feder H M and Sirenko B I 2006 Ecosystem dynamics of the pacific-influenced northern bering and Chukchi Seas in the Amerasian Arctic *Prog. Oceanogr.* **71** 331–61

Kuzyk Z Z A, Gobeil C and Macdonald R W 2013 ^{210}Pb and ^{137}Cs in margin sediments of the Arctic ocean: controls on boundary scavenging *Glob. Biogeochem. Cycles* **27** 422–39

Köseoğlu D, Belt S T, Smik L, Yao H, Panieri G and Knies J 2018 Complementary biomarker-based methods for characterising Arctic sea ice conditions: a case study comparison between multivariate analysis and the PIP_{25} index *Geochim. Cosmochim. Acta* **222** 406–20

Müller J, Masse G, Stein R and Belt S T 2009 Variability of sea-ice conditions in the fram strait over the past 30,000 years *Nat. Geosci.* **2** 772–7

Müller J, Wagner A, Fahl K, Stein R, Prange M and Lohmann G 2011 Towards quantitative sea ice reconstructions in the northern North Atlantic: a combined biomarker and numerical modelling approach *Earth Planet. Sci. Lett.* **306** 137–48

Müller J, Werner K, Stein R, Fahl K, Moros M and Jansen E 2012 Holocene cooling culminates in sea ice oscillations in Fram Strait *Quat. Sci. Rev.* **47** 1–14

Nittrouer C A, Sternberg R W, Carpenter R and Bennet J T 1979 The use of Pb-210 geo chronology as a sedimentary tool: application to the Washington continental shelf *Mar. Geol.* **31** 297–316

Onarheim I H, Eldevik T, Smedsrud L H and Stroeve J C 2018 Seasonal and regional manifestation of arctic sea ice loss *J. Clim.* **31** 4917–32

Pieńkowski A J, Gill N K, Furze M F, Mugo S M, Marret F and Perreaux A 2017 Arctic sea-ice proxies: comparisons between biogeochemical and micropalaeontological reconstructions in a sediment archive from Arctic Canada *Holocene* **27** 665–82

Polyak L, Belt S T, Cabedo-Sanz P, Yamamoto M and Park Y-H 2016 Holocene sea-ice conditions and circulation at the Chukchi-Alaskan margin, Arctic Ocean, inferred from biomarker proxies *Holocene* **26** 1810–21

Robbins J A and Edgington D N 1975 Determination of recent sedimentation rates in Lake Michigan using Pb-210 and Cs-137 *Geochim. Cosmochim. Acta* **39** 285–304

Serreze M C and Stroeve J 2015 Arctic sea ice trends, variability and implications for seasonal forecasting *Phil. Trans. R. Soc.* A **373**

Smik L, Cabedo-Sanz P and Belt S T 2016 Semi-quantitative estimates of paleo Arctic sea ice concentration based on source-specific highly branched isoprenoid alkenes: a further development of the PIP_{25} index *Org. Geochem.* **92** 63–9

Stein R, Fahl K, Schade I, Manerung A, Wassmuth S, Niessen F and Nam S-I 2017 Holocene variability in sea ice cover, primary production, and Pacific-Water inflow and climate change in the Chukchi and East Siberian Seas (Arctic Ocean) *J. Quat. Sci.* **32** 362–79

Stein R, Grobe H and Wahsner M 1994 Organic carbon, carbonate, and clay mineral distributions in eastern central Arctic Ocean surface sediments *Mar. Geol.* **119** 269–85

Stoynova V, Shanahan T M, Hughen K A and de Vernal A 2013 Insights into circum-arctic sea ice variability from molecular geochemistry *Quat. Sci. Rev.* **79** 63–73

Stroeve J, Holland M M, Meier W, Scambos T and Serreze M 2007 Arctic sea ice decline: faster than forecast *Geophys. Res. Lett.* **34** L09501

Taylor K E, Stouffer R J and Meehl G A 2012 An overview of CMIP5 and the experiment design *Bull. Am. Meteorol. Soc.* **93** 485–98

Vare L L, Massé G and Belt S T 2010 A biomarker-based reconstruction of sea ice conditions for the Barents Sea in recent centuries *The Holocene* **40** 637–43

Walsh J E, Fetterer F, Stewart J S and Chapman W L 2016 A database for depicting arctic sea ice variations back to 1850 *Geogr. Rev.* **107** 89–107

Weckström K *et al* 2013 Evaluation of the sea ice proxy IP_{25} against observational and diatom proxy data in the SW Labrador sea *Quat. Sci. Rev.* **79** 53–62

Weingartner T 2006 Circulation, thermohaline structure, and cross-shelf transport in the Alaskan Beaufort Sea *OCS Study MMS 2006-031 Final Report* University of Alaska, Fairbanks p 58

Xiao X, Fahl K, Müller J and Stein R 2015 Sea-ice distribution in the modern Arctic ocean: biomarker records from trans-Arctic ocean surface sediments *Geochim. Cosmochim. Acta* **155** 16–29